Available online at www.sciencedirect.com

ScienceDirect

Procedia Structural Integrity 28 (2020) 1808–1815

Structural Integrity Procedia

www.elsevier.com/locate/procedia

1st Virtual European Conference on Fracture

Multiaxial fatigue life assessment in notched components based on the effective strain energy density

R. Branco[a,*], J.D. Costa[a], L.P. Borrego[b,a], F. Berto[c], J. Razavi[c], W. Macek[d]

[a]*University of Coimbra, CEMMPRE, Department of Mechanical Engineering, 3030-788 Coimbra, Portugal*
[b]*Department of Mechanical Engineering, Coimbra Polytechnic – ISEC, Rua Pedro Nunes, Quinta da Nora, 3030-199 Coimbra, Portugal*
[c]*Department of Mechanical and Industrial Engineering, NTNU, 7491 Trondheim, Norway*
[d]*Opole University of Technology, Prószkowska 76, 45-758 Opole, Poland*

Abstract

This paper presents a methodology to predict the fatigue lifetime in notched geometries subjected to multiaxial loading based on the effective strain energy density concept. The modus operandi consists of defining a fatigue master curve that relates the strain energy density with the number of cycles to failure from standard cylindrical specimens tested under low-cycle fatigue conditions. After that, the multiaxial loading history at the geometric discontinuity is reduced to an equivalent uniaxial loading scenario via the calculation of an averaged value of the strain energy, which is done by combining the equivalent strain energy density concept along with the theory of critical distances. Then, this energy is inserted into the fatigue master curve to estimate the fatigue lifetime. The method is tested in solid round bars with lateral notches subjected to in-phase bending-torsion loading. Overall, the comparison between the experimental and predicted fatigue lives shows a very good agreement. Additionally, the proposed approach enables the determination of the most likely initiation sites as well as the crack angles at the early stage of crack growth.

Keywords: Multiaxial fatigue; bending-torsion; notch effect; strain energy density; fatigue life prediction.

* Corresponding author. Tel.: +351-239790700; fax: +351-239403407.
E-mail address: ricardo.branco@dem.uc.pt

10.1016/j.prostr.2020.11.003

Nomenclature

a_0	El-Haddad parameter
D_{LM}	distance of the Line Method (LM) of the Theory of Critical Distances (TCD)
h	hole depth
F_B	force applied to create the bending moment
F_T	force applied to create the torsion moment
N_i	experimental fatigue life
N_p	predicted fatigue life
σ_a	nominal normal stress amplitude
σ_m	nominal mean normal stress
ΔW_{e^*}	positive component of the elastic strain energy density
ΔW_P	plastic strain energy density
ΔW_T	total strain energy density
$\Delta\sigma_{vM}$	von Mises stress range
$\Delta\sigma_{vM,LM}$	effective value of $\Delta\sigma_{vM}$ calculated using the LM of the TCD

1. Introduction

High-strength steels play an important role in modern automotive industry because of their superior mechanical properties, namely excellent strength-to-weight ratio, high corrosion resistance and low cost (Tisza et al., 2018). Policies to reduce fuel consumption, air pollution and carbon footprint have led to the development of lighter vehicles components (Mayyas et al., 2012). This strategy is often achieved through an optimised design, which may contain abrupt geometrical changes. In the presence of complex cyclic loading, sometimes with a multiaxial nature, these regions are prone to fatigue failure. Therefore, the development of safe and reliable predictive tools is a critical task in fatigue design.

The most efficient multiaxial fatigue models require a huge number of material constants and complex computational simulations, making the process time-consuming and expensive. In the current industrial context, an inefficient strategy of product development is likely to increase the time-to-market and the overall cost, which can be translated into a lack of competitiveness. Thus, there is an urgent need for efficient design solutions, preferably based on simple material characterisation tests, and with high accuracy standards.

The present paper proposes a simple approach to deal with the fatigue behaviour of severely notched components subjected to multiaxial loading. The methodology consists of calculating an effective value of the total strain energy density near the crack initiation site, which is then inserted into a fatigue master curve representative of the elastic-plastic behaviour of the material to account for the fatigue lifetime. The concept is tested in notched round bars with blind transverse holes subjected to in-phase bending-torsion loading. Overall, the predicted lives are very well correlated with those obtained in the experiments.

2. Experimental procedure

The material utilised in this study was the DIN 34CrNiMo6 high-strength steel (Branco et al., 2016). Its main mechanical properties are summarised in Table 1. The specimen geometry used in the multiaxial fatigue campaign, as exhibited in Figure 1, consisted of a solid round bar with a lateral notch. The lateral notch has a U-shaped configuration with a transverse blind hole. The hope depth (h) varied between 0.3 and 1.4 mm (see Table 2). The tests were conducted under pulsating conditions, in a conventional servo-hydraulic machine connected to a custom-made gripping system. Three bending moment to torsion moment (B/T) ratios and three levels of nominal stress were used (see Table 2). Notch surfaces were observed in-situ using a high-resolution digital camera and an optical device with variable magnification. Images were periodically recorded through a PC-based data acquisition system.

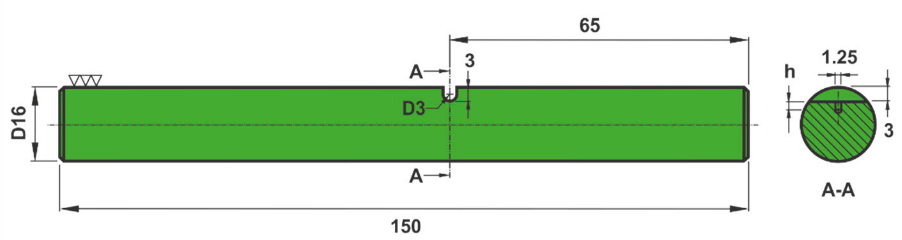

Fig. 1. Specimen geometry used in the multiaxial fatigue campaign: (a) first picture; (b) second picture.

Table 1. Mechanical properties of the DIN 34CrNiMo6 high strength steel.

Mechanical property	Value
Yield strength, σ_{YS} (MPa)	967
Tensile strength, σ_{UTS} (MPa)	1035
Young's modulus, E (GPa)	209.8
Poisson's ratio, ν	0.296
Coefficient κ_t [MJ/m^3]	2165.37
Exponent α_t	-0.6854
Constant ΔW_{0t} [MJ/m^3]	0.7049
Stress intensity factor range threshold, ΔK_{th0} (MPa·m$^{0.5}$)	7.12

Table 2. Summary of the multiaxial fatigue testing campaign.

B/T	D (mm)	h (mm)	σ_a (MPa)	σ_m (MPa)	N_i (cycles)	N_p (cycles)
			$\sigma_a/\tau_a=4$, $\sigma_m/\tau_m=4$			
2	16	0.3	224	239	10,557	10,313
2	14	0.6	179	194	17,111	10,466
2	14	0.3	179	194	59,878	39,417
			$\sigma_a/\tau_a=2$, $\sigma_m/\tau_m=2$			
1	16	1.3	224	239	2406	1733
1	14	0.5	179	194	15,320	8230
1	14	1.4	298	313	1250	953

3. Numerical procedure

The stress and strain fields at the notch region were computed via three-dimensional numerical models. Meshes were developed in a parametric framework using 8-node isoparametric brick elements assuming a homogeneous, linear-elastic, and isotropic material. Figure 2 shows the finite element mesh developed in this study. At the geometric discontinuity, the mesh was carefully refined (Figure 2(b)) while, at remote regions, a coarser pattern was adopted. The assembled model had 89,584 elements and 97,704 nodes.

The loading scenarios were replicated by two pairs of forces placed at one end of the specimen, while the other end was fixed. Torsion moments were created by the F_T forces applied on a plane normal to the longitudinal axis of the specimen with opposite directions. Bending moments were created by the F_B forces applied parallelly to the longitudinal axis of the specimen but with opposite directions. The relationship between the normal and shear stresses was established by adjusting the value of the λ, i.e. λ=1/2 and λ=1 for B/T=2 and B/T=1, respectively.

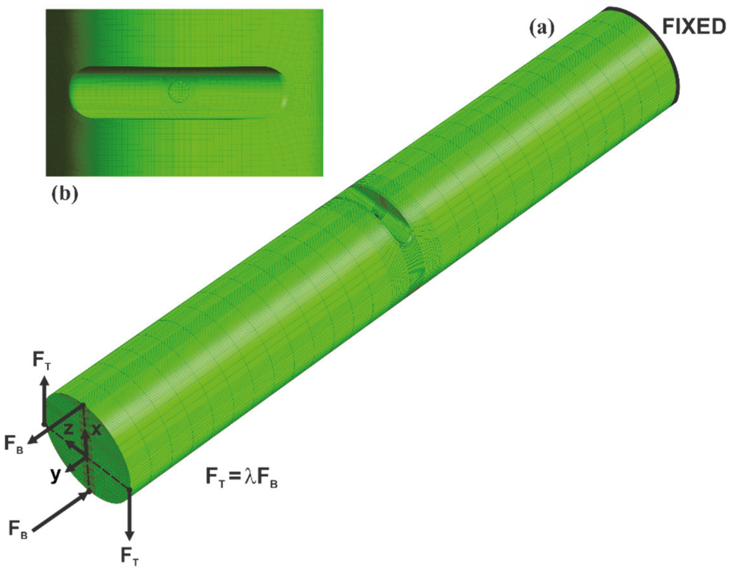

Fig. 2. Three-dimensional finite-element mesh: (a) assembled model; (b) detail of the notch region.

4. Results and discussion

4.1. Multiaxial fatigue behaviour

Multiaxial fatigue design is a complex task. One of the critical issues is the identification of the crack initiation sites. Figure 3 shows typical examples observed in the experiments for the different B/T ratios. In this geometry, the fatigue process is characterised by the nucleation of two cracks, in diametrically opposite points, whose locations are governed by the loading scenario. It is clear from the figure that the higher the B/T ratio, the higher the angle formed by the line joining the two initiation sites and the vertical axis. This can be explained by the lower shear stress levels associated with increasing B/T ratios making the propagation closer to mode-I loading. These trends were confirmed numerically assuming that crack initiation sites occur at the points with the maximum values of the first principal stress. The squares, which represent the predicted initiation sites, are quite close to the experimental observations.

The trajectory described by a crack when subjected to specific loading history is a relevant matter in the context of mechanical design. Its accurate prediction is not a trivial subject, particularly under multiaxial loading. Figure 3

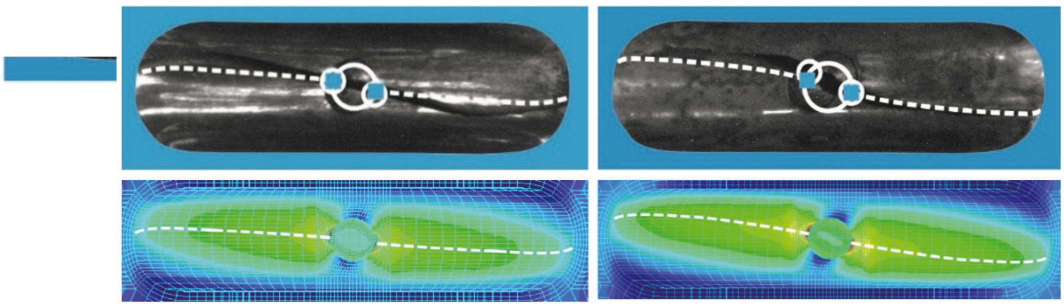

(a) **(b)**

Fig. 3. Macroscopic appearance of the fracture surfaces and first principal stress fields at the notch region for: (a) B/T=2; and B/T=1. Dashed lines represent the predicted surface crack paths. White circles represent the predicted crack initiation sites. Squares represent the experimental crack initiation sites.

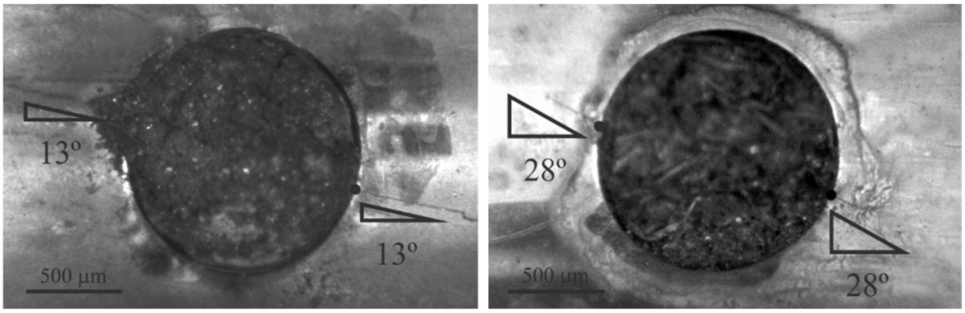

(a) **(b)**

Fig. 4. Experimental surface crack angles at the early stage of growth: (a) B/T=2; and (b) B/T=1. Numerical predictions obtained from the first principal direction at the crack initiation site.

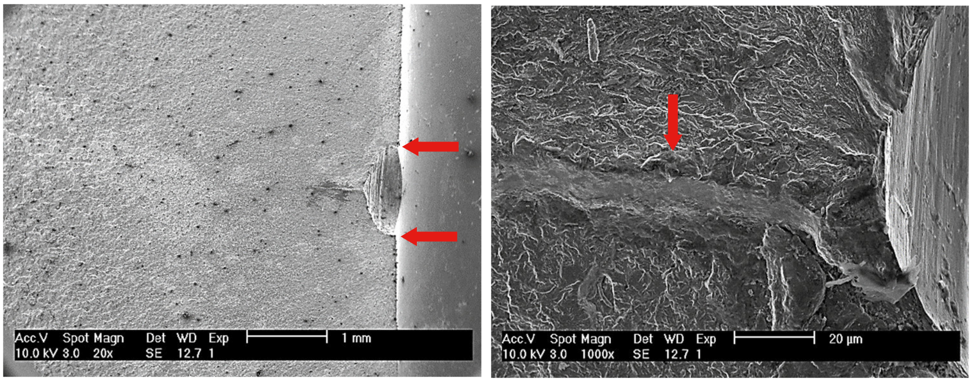

(a) **(b)**

Fig. 5. SEM images of samples subjected to B/T=2: (a) overall aspect of fracture surface near the initiation sites (identified by the arrows); and (b) magnification of fracture surface near the blind hole.

shows representative surface crack paths observed in the experiments. The surface crack paths are remarkably affected by the multiaxial loading history. Overall, the increase of the B/T ratio leads to straighter surface trajectories. This can be explained by the smaller shear stress levels, which reduce the degree of mixed-mode propagation.

Regarding the fatigue crack initiation angles, literature suggests an important role of the loading scenario, either under in-phase or out-of-phase conditions (Lopez-Crespo et al., 2015). The experimental measurements, as indicated in Figure 4, show that the fatigue crack angles at the early stage of growth decrease with increasing values of the B/T ratio. Higher B/T ratios reduce the predominance of shear stresses and, therefore, the crack front tends to be closer to mode-I. In addition, it is interesting to note that the angles of the two diametrically opposite cracks are relatively similar.

The fatigue damage mechanisms associated with the failure process can be distinguished in Figure 5. As can be seen, there is the nucleation of two cracks at the hole border (identified by the arrows in Figure 5(a)) caused by the highest stress concentrations acting in such places (see Figure 3). The fatigue step visible in Figure 5(b) is the result of the coalescence of the two cracks. A close look at this region shows traces of plastic deformation, namely fatigue striations with radial orientation, which denotes a ductile failure mode. Additionally, there is a population of non-metallic particles disperse throughout the fracture surfaces (see Figures 5(a)).

4.2. Multiaxial fatigue life prediction

The fatigue design of engineering components subjected to multiaxial loading histories is a challenging issue and has inspired the development of different prediction proposals, which are usually organised into stress-based, strain-based, energy-based, and critical plane-based models (Socie et al, 2000). The presence of severe notches makes the problem more difficult. Currently, there are different theories to deal with the notch effect (Liao et al., 2020).

Here, a straightforward model is proposed to evaluate the fatigue life in notched components subjected to proportional loading (Branco et al., 2018b). Two main assumptions are assumed as a starting point: (1) regardless of the geometric discontinuity, fatigue life is the same, if the stress-strain histories at the initiation sites are similar; and (2) fatigue failure occurs when a critical value of strain energy density is reached at the initiation site.

The modus operandi consists of four main tasks (see Figure 6): (1) reduction of the multiaxial stress state to an equivalent uniaxial stress state; (2) computation of an effective stress at the fatigue process zone; (3) calculation of an effective value of the total strain energy density (ΔW_T) defined by the sum of both the elastic positive and plastic components using the ESED concept (Glinka et al., 1988); and (4) prediction of crack initiation life from a fatigue master curve defined from smooth specimens subjected to uniaxial strain-controlled conditions.

In the current approach, the reduction of the multiaxial stress state to the equivalent uniaxial stress state was done by means of the von Mises stress range. The effective stress range was evaluated at the initiation site, in the critical direction, using the Line Method of the Theory of Critical Distances. Figure 7 shows typical evolutions of the von Mises stress range, in a dimensionless form, with the distance from the notch surface, normalised by critical distance, for the cases studied here. Overall, these functions are affected by the B/T ratio and the hole depth. However, near the notch surface, these dimensionless functions are relatively similar.

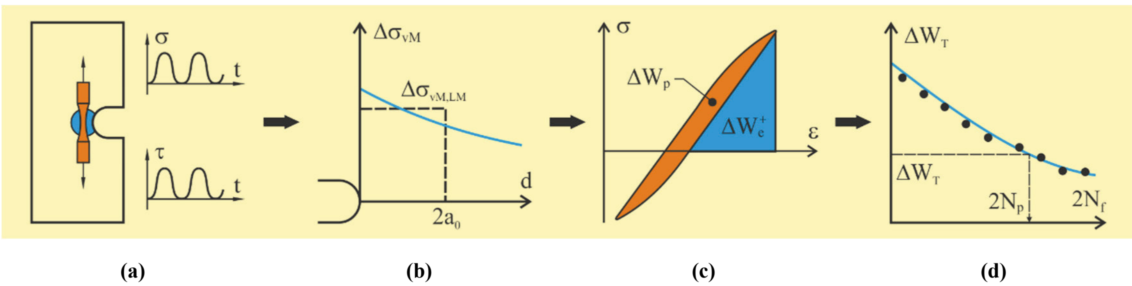

Fig. 6. Schematic representation of the predictive model employed to estimate the fatigue crack initiation lifetime.

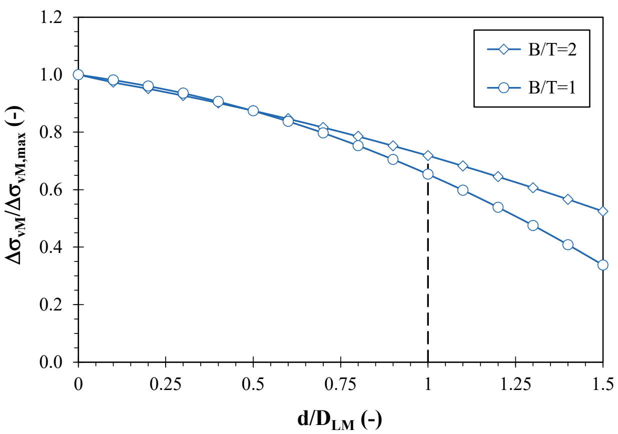

Fig. 7. Dimensionless local von Mises stress range against the distance from the notch surface at the initiation site for different BT ratios.

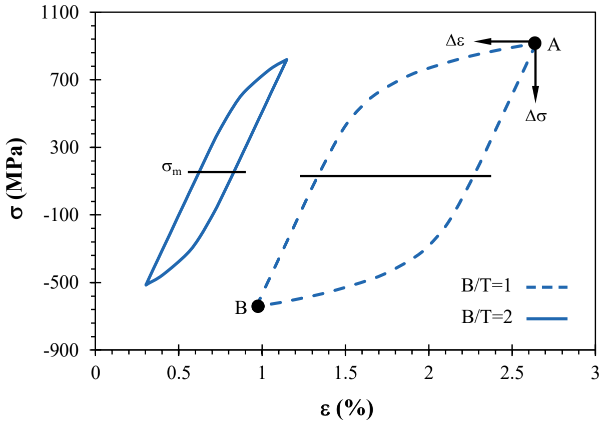

Fig 8. Stress-strain circuits generated using the ESED concept from an effective value of the von Mises stress range computed using the Theory of Critical Distances.

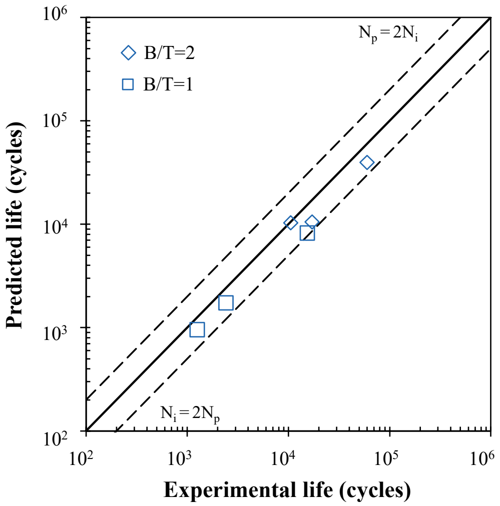

Fig. 9. Experimental fatigue crack initiation life versus numerical predictions computed using the TSED approach.

The stress-strain hysteresis loops were generated by means of the ESED concept. Figure 8 exhibits examples of the stable loops generated is this study for different loading scenarios. As shown, the plastic strain varies with the B/T ratio, and also the geometric discontinuity (Branco et al. 2018b). The generated loops were then used to calculate the corresponding value of the total strain energy density, defined as the sum of the plastic component and the elastic positive component, at the notch-controlled process zone.

The final step consisted of calculating the fatigue crack initiation lifetime. The effective value of the total strain energy density was inserted into the fatigue master curve to estimate the number of cycles to failure (N_p):

$$\Delta W_T = \alpha_T (2N_f)^{\kappa_t} + \Delta W_{0T} \quad (1)$$

where the constants for the studied alloy are listed in Table 2. Figure 9 compares the predicted lives (N_p) with those obtained in the experiments (N_i) for the different loading scenarios. Here, the experimental fatigue life, listed in Table 2, was defined for a crack length equal to the material characteristic length, defined from the El-Haddad parameter (a_0). For this alloy, at pulsating loading conditions, a_0 = 129 µm (Branco et al., 2018b). As can be seen, the results are within scatter bands of two, which is a very interesting outcome. A closed analysis shows that predictions are tendentially conservative, which is also quite interesting.

5. Conclusions

The present paper studied the multiaxial fatigue behaviour of round bars with blind holes subjected to multiaxial loading. Fatigue life assessment was carried out using the effective value of the strain energy density computed at the initiation site within a linear-elastic framework. The following conclusions can be drawn:

(1) Fatigue failure was characterised by the initiation and growth of two cracks at diametrically opposite sites around the hole surface. Both the crack initiation sites as well as the crack angles at the early stage of growth were significantly affected by the bending-to-torsion ratio;

(2) Fatigue crack initiation sites and fatigue crack angles at the early stage of growth were successfully predicted from the maximum value of the first principal stress and from the first principal direction at the initiation site, respectively;

(3) Fatigue life was estimated via an effective value of the total strain energy density evaluated near the crack initiation site with Line Method of the theory of critical distances along with the Equivalent Strain Energy Density concept.

(4) Fatigue life predictions were very well correlated with the experimental observations obtained in severely notched round bars containing lateral U-shaped notches with blind transverse holes and subjected to different B/T ratios and nominal stress levels.

Acknowledgements

This research is sponsored by FEDER funds through the program COMPETE – Programa Operacional Factores de Competitividade – and by national funds through FCT – Fundação para a Ciência e Tecnologia – under the project UIBD/00285/2020.

References

Branco, R., Costa, J.D., Antunes, F.V., Perdigão, S., 2018. Monotonic and cyclic behavior of DIN 34CrNiMo6 tempered alloy steel. Metals, 6(5), 98, doi: 10.3390/met6050098.

Branco, R., Prates, P., Costa J.D., Berto, F., Kotousov, A., 2018b. New methodology of fatigue life evaluation for multiaxially loaded notched components based on two uniaxial strain-controlled tests. International Journal of Fatigue 111, 308–320, doi: 10.1016/j.ijfatigue.2018.02.027.

Glinka, G., Ott, W., Nowack, H., 1988. Elastoplastic plane strain analysis of stresses and strains at the notch root. Journal of Engineering Materials and Technology 110, 195-204, doi:10.1115/1.3226037

Liao, D., Zhu, S.P., Correia, J.A.F.O., de Jesus, A.M.P., Berto, F., 2020. Recent advances on notch effects in metal fatigue: A review. Fatigue and Fracture of Engineering Materials and Structures 43, 637-659, doi:10.1111/ffe.13195.

Lopez-Crespo, P., Moreno, B., Lopez-Moreno, A., Zapatero, J., 2015. Study of crack orientation and fatigue life prediction in biaxial fatigue with critical plane models. Engineering Fracture Mechanics 136, 115-130, doi:10.1016/j.engfracmech.2015.01.020.

Mayyas, A., Qattawi, A., Omar, M., Shan, D. 2012. Design for sustainability in automotive industry: A comprehensive review. Renewable and Sustainable Energy Reviews 16, 1845-1862, doi: 10.1016/j.rser.2012.01.012.

Socie, D., Marquis, G., 2000. Multiaxial Fatigue. Society of Automotive Engineers, ISBN: 0-7680-0453-5.

Tisza, M., Czinege, I., 2018. Comparative study of the application of steels and aluminium in lightweight production of automotive parts. International Journal of Lightweight Materials and Manufacture, 1, 229-238, doi: 10.1016/j.ijlmm.2018.09.001.